Chapter 20
Fluorescence Recovery After Photobleaching (FRAP) to Study Nuclear Protein Dynamics in Living Cells

Martin E. van Royen, Pascal Farla, Karin A. Mattern, Bart Geverts, Jan Trapman, and Adriaan B. Houtsmuller

Keywords Fluorescence recovery after photobleaching; FRAP; Protein mobility; Confocal microscopy; Androgen receptor; Fluorescent proteins

Abstract Proteins involved in chromatin-interacting processes, like gene transcription, DNA replication, and DNA repair, bind directly or indirectly to DNA, leading to their immobilisation. However, to reach their target sites in the DNA the proteins have to somehow move through the nucleus. Fluorescence recovery after photobleaching (FRAP) has been shown to be a strong approach to study exactly these properties, i.e. mobility and (transient) immobilisation of the proteins under investigation. Here, we provide and discuss detailed protocols for some of the FRAP procedures that we have used to study protein behaviour in living cell nuclei. In addition, we provide examples of their application in the investigation of the androgen receptor (AR), a hormone-inducible transcription factor, and of two DNA-maintenance factors, the telomere binding proteins TRF1 and TRF2. We also provide protocols for qualitative FRAP analysis and a general scheme for computer modelling of the presented FRAP procedures that can be used to quantitatively analyse experimental FRAP curves.

1 Introduction

1.1 Green Fluorescent Protein

In the past decade, genetic labeling with fluorescent proteins has caused a revolution in molecular cell biological research. Ever since they became available, green fluorescent protein (GFP) and its color variants have been used at a tremendous scale to study the dynamic behavior of proteins in their most natural environment, the living cell. GFP was derived from the jellyfish *Aequorea Victoria* ***(1)***. By mutagenesis of wild-type GFP, enhanced versions, such as enhanced GFP (EGFP) with improved brightness and expression properties have been developed

R. Hancock (ed.) *The Nucleus: Volume 2: Chromatin, Transcription, Envelope, Proteins, Dynamics, and Imaging*,

© Humana Press 2008

(reviewed in ref. ***(2)***). In addition, currently a large array of color variants has been generated (reviewed in refs. ***(3, 4)***). GFP and its color variants provide minimally invasive tools, not only to determine the dynamic intracellular localization using e.g. confocal time-lapse imaging, but also to study the dynamic behavior of proteins in living cells (reviewed in ref. ***(5)***).

1.2 Fluorescence Recovery After Photobleaching (FRAP)

Proteins involved in DNA-interacting processes, like DNA repair, DNA replication, and transcription, bind directly or indirectly to DNA to exert their function. To reach their target sites in the DNA, either DNA damage, replication origins, or transcription sites, nuclear proteins have to move through the nucleus. Fluorescence recovery after photobleaching (FRAP) has proven to be a strong approach to qualitatively or quantitatively study exactly these properties, i.e. the mobility and (transient) immobilization of molecules in living cells (***(6–12)***, and reviewed in ref. ***(13)***). FRAP was developed in the 1970s by Axelrod and coworkers. Early FRAP investigations were focused on the mobility of fluorescently labelled constituents of the cell membrane ***(14)***. The development in the 1980s and 1990s of confocal microscopy and GFP technology enormously enhanced the applicability of FRAP. Currently, by far the most FRAP studies use confocal microscopes, although widefield systems are also becoming increasingly available (e.g. ref. ***(15)***).

In a typical FRAP experiment, a small defined region within a larger volume (for instance the cell nucleus) is shortly illuminated at high laser intensity (Fig. 20.1a) ***(13)***. Immediately after the bleach-pulse the majority of the GFP-tagged proteins within the region have irreversibly lost their fluorescent properties, a process referred to as photobleaching. In a situation where all GFP-tagged proteins are mobile, proteins from outside will diffuse into the bleached region resulting in an increase of the fluorescent signal in the region until the signal inside the bleached region is equal to the signal outside the bleached region. In contrast, if permanently immobile proteins are present, these will not diffuse into the strip, resulting in an incomplete recovery of the fluorescent signal inside the bleached region relative to the remainder of the nucleus (Fig. 20.1b) (*see* **Note 1**). Transient immobilization, as was observed for many active nuclear proteins, including the AR, results in a delayed, secondary fluorescence recovery in the bleached region because a fraction of immobilized proteins will release and become mobile during the FRAP experiment, and then contribute to fluorescence recovery but later than the mobile fraction (Fig. 20.1) ***(13)***. Summarizing, FRAP experiments yield information on essentially three mobility parameters: diffusion coefficient, immobile fraction, and the time spent in the immobile state. Assuming elementary binding kinetics, the size of the immobile fraction and the duration of immobilisation are determined by the on- and off-rates of the investigated protein to and from immobile complexes (*see* **Note 2**).

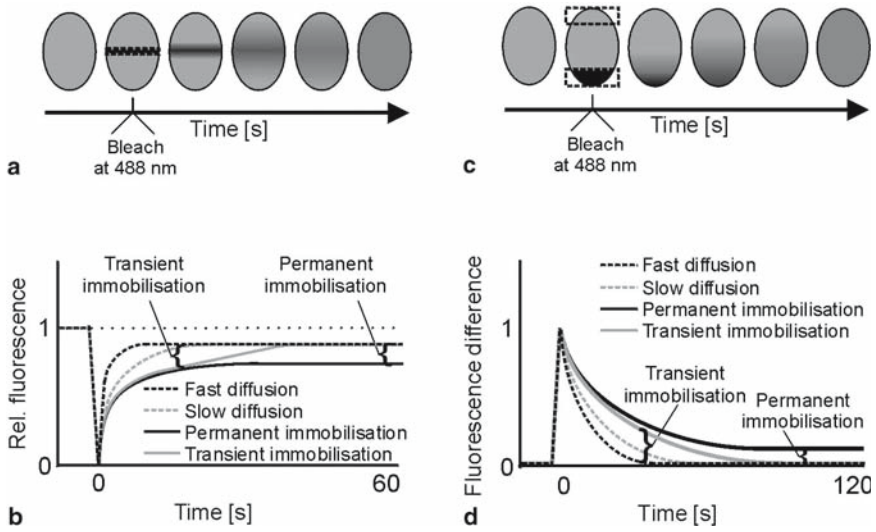


Fig. 20.1 Schematic representation of the principles of strip-FRAP and combined FLIP-FRAP. **a** In strip-FRAP, the recovery of GFP fluorescence is recorded in time after shortly bleaching a small strip spanning the nucleus. **b** Strip-FRAP curves representing different scenarios are expressed relative to pre-bleach values and the intensity directly after bleaching. Permanent immobilization of GF-tagged proteins (*solid curve*) can be identified by an incomplete recovery compared to FRAP curves of molecules that are freely mobile (*dotted curve* with fast diffusion and *dotted grey curve* with slow diffusion). Transient immobilization leads to a secondary recovery of fluorescence (*solid grey curve*). **c** In FLIP-FRAP experiments, the fluorescence in the bleached region and in the region at the opposite nuclear pole are recorded in time after photobleaching until a new steady state is reached. **d** The differences in fluorescence between the two opposite poles identify the different scenarios. Similar to strip-FRAP, a permanent immobilisation results is an incomplete redistribution and thus a constant difference between both signals in the two measured regions

Several variants of FRAP have been developed, including spot-FRAP, strip-FRAP, fluorescence loss in photobleaching (FLIP) ***(16)***, combined FLIP-FRAP ***(6, 7, 17, 18)*** and inverted FRAP (iFRAP) ***(19)***. Spot-FRAP is based on photobleaching of a small spot whereas in strip-FRAP, a larger region, for instance a narrow strip spanning the nucleus, is bleached. The latter method is favourable when signals are very low, e.g. due to low expression of the GFP-tagged protein. In FLIP, a very common variant of FRAP, the loss of fluorescence in a region or structure distant from the bleached region is monitored. FRAP and FLIP can also be combined (FLIP-FRAP): two regions at two poles of an ellipsoid nucleus are monitored simultaneously after bleaching only one of them. FLIP and combined FLIP/FRAP are specifically useful to determine the residence time of proteins inside subnuclear structures, such as telomeres, repair foci, or speckles. In iFRAP the entire nucleus is bleached with exception of a structure of interest. Immediately after bleaching, loss of fluorescence in the structure fully represents the off-rate of the associated protein (*see* **Note 3**).

1.3 Application of FRAP to Proteins in the Living Cell Nucleus

Application of FRAP to investigate the dynamic behaviour of nuclear proteins has provided new insights in nuclear protein function. The first FRAP studies revealed an unexpected high mobility of many nuclear factors, including components of the nucleotide excision repair (NER) machinery, which removes certain types of single-strand DNA damage ***(20–24)***, transcription factors ***(9)***, and RNA-splicing factors ***(25)***. It was shown that in the absence of DNA damage the NER-factors ERCC1/XPF ***(20)***, XPA ***(21)***, PCNA ***(22, 23)***, and recently XPG ***(24)*** were highly mobile in living cells and bound transiently to DNA damage. Similarly, high mobility and transient immobilisation due to DNA-binding were found for steroid receptors (***6, 9)*** and for many more nuclear proteins with roles in a diversity of other processes ***(26)***, including double-strand break repair ***(27–30)***, DNA replication ***(22, 23, 31)***, chromatin structure ***(18, 32–34)***, and RNA processing and transcription ***(19, 25, 34–36)***.

1.4 Examples of FRAP Applications: Androgen Receptors and Telomere-Binding Proteins

In this chapter, we provide detailed procedures for two types of FRAP, strip-FRAP and combined FLIP-FRAP, to study the dynamic behavior of the androgen receptor (AR) and give an example of a investigation of the telomere-binding proteins TRF1 and TRF2. We also provide methods to qualitatively analyze FRAP curves (Fig. 20.2) as well as an elementary modelling algorithm to generate FRAP curves with varying mobility parameters to fit and quantify the experimental data (Fig. 20.3).

The AR is a hormone-induced transcription factor and a member of the nuclear receptor (NR) superfamily. The AR is involved in the development and maintenance of the male phenotype and also plays a crucial role in the development and progression of prostate cancer ***(37, 38)***. Like all NRs the AR consists of three domains: a conserved DNA-binding domain (DBD), a C-terminal ligand-binding domain (LBD), and a more variable N-terminal domain (NTD) (***39***). Ligand-activated ARs translocate to the nucleus where they exert their activity by binding to specific androgen response elements (AREs) in promoter and enhancer sequences of AR-regulated genes ***(40, 41)***. Several FRAP studies show a high mobility and transient immobilization not only of the AR but also of other NRs (Fig. 20.4) ***(6–9, 11, 42, 43)***.

This immobilization is lost in a non-DNA-binding AR mutant (AR A573D) ***(6, 44)*** and in wild-type AR in the presence of antagonists ***(7)***. In FRAP experiments direct comparison of active versus inactive states, like DNA repair proteins in the presence or absence of DNA damage or non-DNA binding transcription factor mutants in transcription, greatly simplifies the interpretation of the generated data. Computer simulation-aided analysis of combined experimental strip-FRAP and FLIP-FRAP data (Fig. 20.4a–d) showed that the wild-type AR kinetics could not be described by a model of freely diffusing molecules only (Fig. 20.4e, f). A model

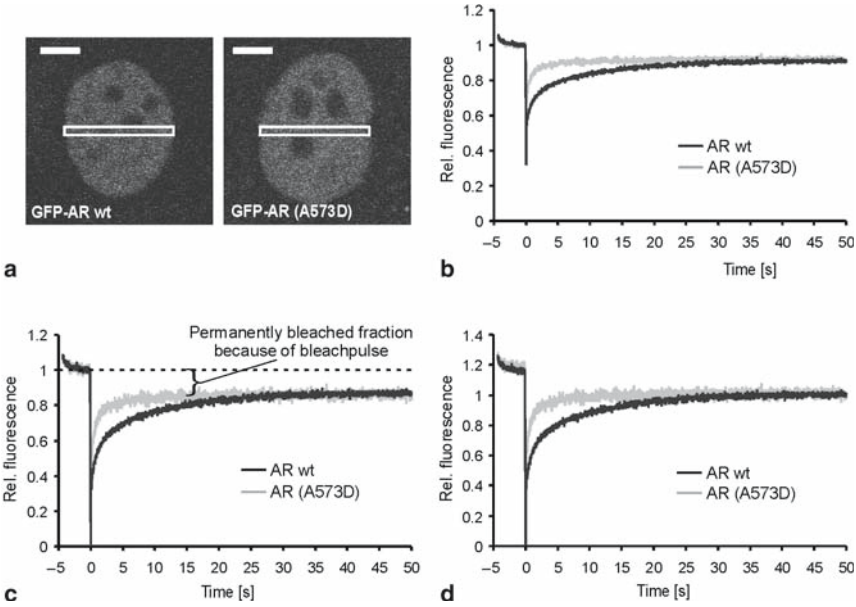


Fig. 20.2 Strip-FRAP applied to wild-type and mutant ARs. **a** and **b** Confocal images of Hep3B cells stably expressing GFP-AR (wild type) or the DNA binding-deficient mutant, GFP-AR (A573D) (**a**) and their strip-FRAP curves normalised by the three different normalisation procedures given in **Section 3.4.3. b–d** Bar, 5 µm. The recovery of fluorescence in a small strip spanning the nucleus (*white box* in **a**) is recorded in time after shortly photobleaching the fluorescence. **b** The most straightforward normalisation procedure is to normalise the data relative to pre-bleach fluorescence intensities. Comparing normalised data of active versus inactive proteins like wild-type AR and AR (A573D) used here enables identification of transient and permanent immobilisation. The wild-type AR shows a slower total recovery of fluorescence compared with the non-DNA-binding mutant, AR (A573D), due to transient immobilisation of wild-type AR. The difference in intensity of the DNA binding-deficient AR (A573D) before and after complete recovery does not reflect a permanent immobilisation, but is caused by the permanent bleaching of a fraction of protein by the bleach pulse. Curves represent data of at least 10 cells. *Rel*, relative. **c** Applying a second normalisation procedure, correcting possible variations in bleach-depths, data is expressed relative to pre-bleach intensities and the intensity directly after bleaching. The difference between pre-bleach intensity and the intensity after complete redistribution of AR (A573D) reflects the fraction permanently bleached due to the bleach pulse. **d** A third way of normalization yields a curve running from 0 directly after bleaching, to 1 after complete recovery, allowing also quantitative analysis by fitting the data to any equation that represents the diffusion process (and transient immobilization) ***(13)***. After this normalization, it is no longer possible to extract information on permanent immobilization (**Section 3.4.3**)

of freely diffusing molecules together with a transiently immobilized fraction fitted to both strip-FRAP and FLIP-FRAP curves (Fig. 20.4g, h) ***(7)***.

A second example of FRAP application concerns the investigation of telomere-binding proteins. Telomeres are nucleoprotein structures at chromosome ends. Telomere-binding proteins play a key role in the regulation of the length of the telomeric DNA tract. In addition these proteins prevent end-to-end fusion of

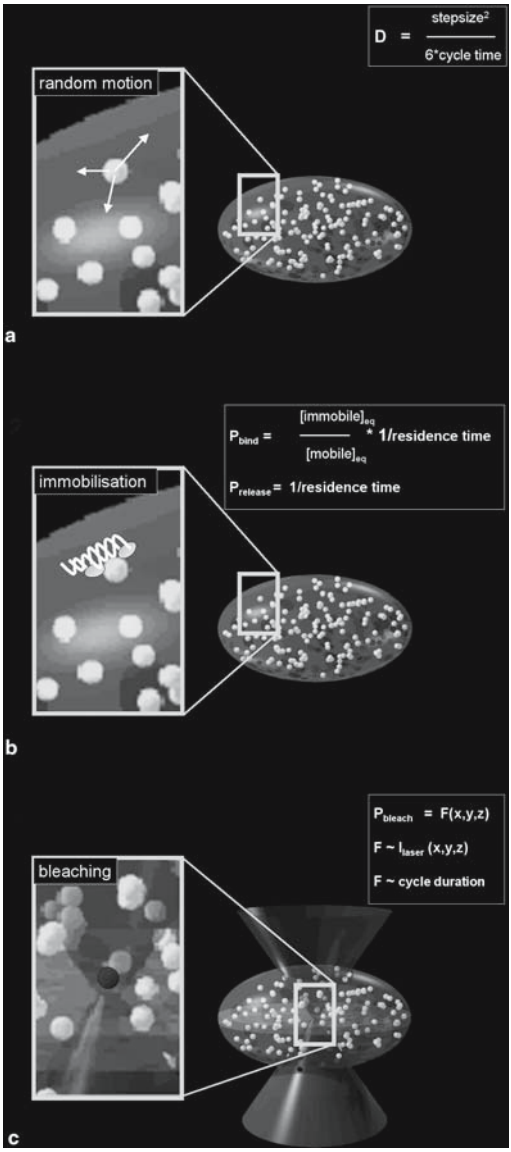


Fig. 20.3 General scheme for Monte Carlo simulation of FRAP on nuclear proteins. **a** Schematic drawing of a cell nucleus (*ellipsoid*) containing randomly distributed GFP-tagged proteins (*spheres*). Random Brownian motion (*inset*) is simulated on the basis of the Einstein-Smoluchowsky equation D = stepsize^2/6* cycle time (*see* **Section 3.4.4**). **b** Simulation of binding to randomly distributed immobile target sites in the DNA (*inset*) is simulated by evaluating a chance to bind or to release based on simple binding kinetics, where the ratio between on- and off-rates (defined by k_{on} and k_{off}, *see* **Section 3.4.4**) equals the ratio between the number of immobile and mobile molecules. **c** Photobleaching is simulated by evaluating a chance to get bleached based on the intensity profile of the laser beam. This profile can be obtained experimentally by illuminating a paraformaldehyde-fixed nucleus with a stationary laser beam at different intensities and collecting 3-D image stacks afterwards. Also GFP-blinking can be simulated (*see* **Note 25**)

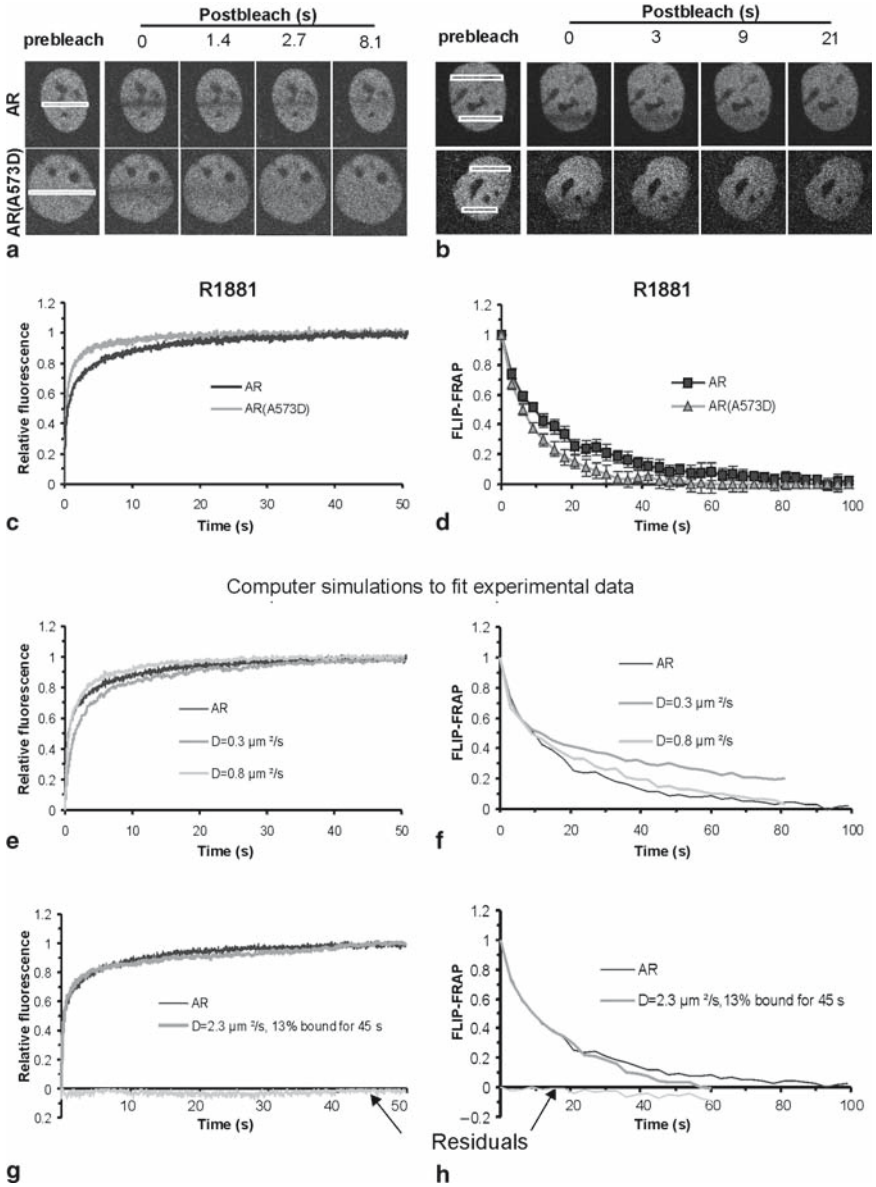


Fig. 20.4 Combined strip-FRAP and FLIP-FRAP reveal that a fraction of agonist-liganded GFP-ARs is transiently immobilized. **a** In the strip-FRAP procedure a strip in the centre of a nucleus is bleached (*rectangle*) at high laser power. Subsequently, fluorescence in the strip is measured at regular time intervals. **b** In the FLIP-FRAP procedure a strip at one pole of the nucleus was bleached for a relatively long period. The difference between fluorescence signals in the bleached region (FRAP, *lower rectangle*) and a distal region at 10 μm from the bleached region of the nucleus (FLIP, *upper rectangle*) was determined at regular time intervals. **c**, **d** Strip-FRAP and FLIP-FRAP experiments of GFP-AR or the non-DNA-binding mutant GFP-AR(A573D) in the

chromosomes. Application of FRAP to two telomeric proteins (TRF1 and TRF2) revealed that telomere binding occurs in a complex dynamic fashion (Fig. 20.5).

2 Materials

2.1 Constructs

1. Standard EGFP, EYFP, and ECFP vectors for cloning (Clontech, Palo Alto, CA, USA) (*see* **Note 4**).
2. pAR0, expressing human full-length wild-type AR ***(39)***, is used to fuse the AR with the fluorescent proteins.
3. pGEM-T-Easy (Promega, Madison, WI, USA).

2.2 Cell Culture and Transfection

1. Hep3B human hepatocellular carcinoma cell line (ATCC HB-8064; LGC Promochem, Teddington, UK) (*see* **Note 5**).
2. Alpha Minimal Essential Medium (αMEM) (Bio-Whittaker/Cambrex, Verviers, Belgium) supplemented with 2 m*M* L-glutamine (Bio-Whittaker/Cambrex), 100 U/mL of penicillin, 100 µg/mL of streptomycin (Bio-Whittaker/Cambrex) and 5% v/v triply 0.1-µm sterile-filtered fetal bovine serum (FBS) (HyClone, South Logan, UT, USA). Store at 2–8°C.

Fig. 20.4 (continued) presence of an agonistic ligand (10^{-9} *M* R1881). **c** Graph showing fluorescence intensities relative to complete redistribution of the non-DNA-binding mutant GFP-AR(A573D) in the presence of R1881 plotted as a function of time. Mean values of at least 10 cells are plotted. All experiments were performed at least three times. **d** Graph showing the difference between fluorescence intensity in the FLIP and FRAP regions (*rectangles* in **b**) relative to the difference directly after bleaching, plotted against time. Mean values ±2× the SEM of two independent experiments on at least ten cells are plotted. **e**, **f** Computer simulations of strip-FRAP and FLIP-FRAP of freely diffusing molecules do not explain the experimental FRAP data obtained with both methods. Experimental strip-FRAP data on wild-type GFP-AR lies in between curves representing the indicated scenarios of free diffusion (**e**), whereas experimental FLIP-FRAP data on wild-type GFP-AR lies outside these boundaries (**f**). **g**, **h** Computer simulations representing a model where, next to freely diffusing molecules, a fraction is transiently immobilized, fitted both strip-FRAP and FLIP-FRAP experimental curves on wild-type GFP-AR. Computer simulations correspond to the average of best fits of FRAP and FLIP-FRAP experiments respectively, so are not necessarily the best fits of the individual experiments. Absolute value of residuals of the computer simulation fit and the experimental data on each time point are plotted below the *x*-axis. (Figure adapted from ref. ***(7)***)

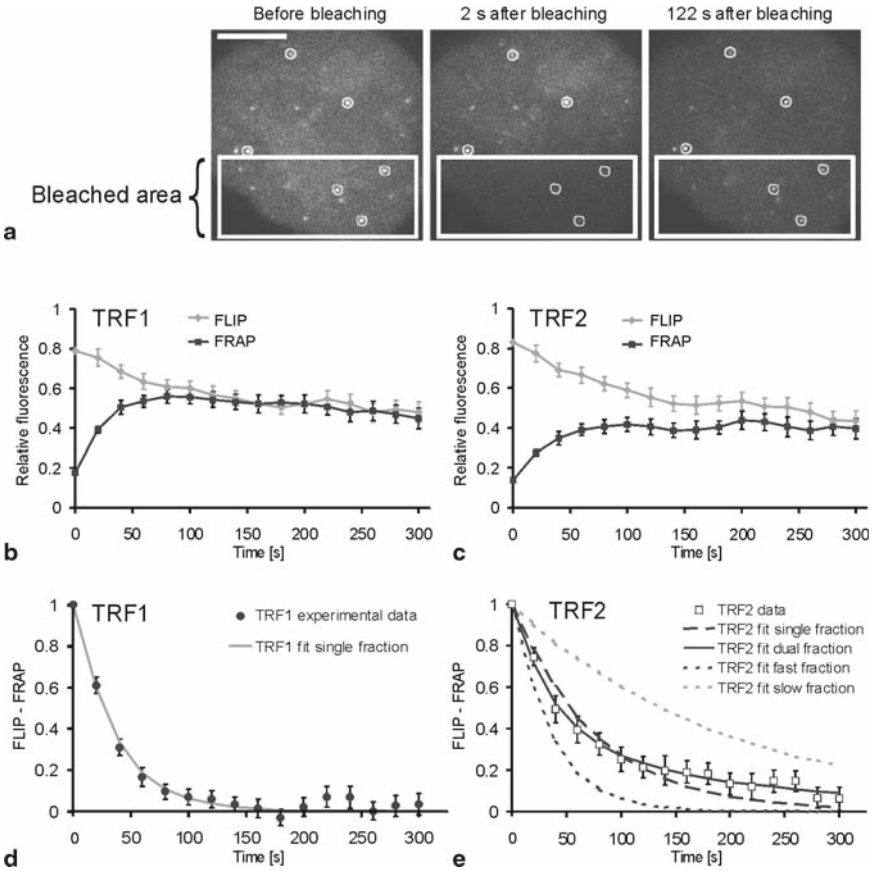


Fig. 20.5 Simultaneous FLIP-FRAP of telomere-bound proteins TRF1 and TRF2. **a** FLIP-FRAP on living HeLa cells expressing GFP-TRF1. Cells are photobleached over a region covering about one half of the nucleus (indicated by a *white box*). The images were acquired before bleaching and at 20-sec intervals after bleaching, starting at 2 sec. The *circles* in the bleached area and unbleached area indicate the regions that are used to calculate fluorescence redistribution. Scale bar, 5 µm. **b**, **c** Quantitative analysis of redistribution of GFP-TRF1 (**b**) and GFP-TRF2 (**c**) at telomeres separately in bleached (in *white box*) and unbleached (*upper*) half of the nucleus. Values are means ± SEM from at least 40 cells. (**d**) Difference (Δ) in telomere intensity in bleached and unbleached parts of the cell, calculated from the data shown in **b** (TRF1) and **c** (TRF2). **e** A fitting analysis of the experimental data in **d** to the equation $\Delta I_{rel}(t) = f_1 e^{-k_1 t} + f_2 e^{-k_2 t}$ indicated a good fit with the single binding kinetics of GFP-TRF1 (*solid grey line*). In contrast, GFP-TRF2 redistribution does not fit with single binding kinetics (*dotted black line*) but does fit with dual binding kinetics (*solid black line*). Note the similarity between the fitted curves of the fast fraction of TRF2 and of TRF1. (Figure adapted from ref. (18))

3. G418 sulfate (Geneticin) (HyClone): working solution is 100 mg/mL active concentration in PBS. Final concentration in culture medium is 0.6 mg/mL of G418 (*see* **Note 6**).

4. Methyltrienolone (R1881; NEN DuPont, Boston, USA): dissolve in EtOH to 1 m*M* stock solution. The stock solution is diluted stepwise (1:10) in EtOH down to 1 n*M* R1881 to generate an array of working solutions. For our experiments we used the 1 μ*M* working solution to obtain a final concentration of 1 n*M* of hormone in our culture medium. R1881 is light-sensitive and stored at −18°C.
5. Charcoal-stripped serum (Hyclone, or can be prepared by a protocol such as that described at www.sigmaaldrich.com/sigma/usage/f2442use.pdf).
6. Trypsin-EDTA (Bio-Whittaker/Cambrex): contains 200 mg/mL of Na_4EDTA, 500 mg/L of trypsin 1:250. Sterile filtered. Store the stock solution at −10°C and the working solution at 2–8°C.
7. Cover slips: 24-mm diameter, 0.13–0.16 mm thickness (Menzer-Gläser/Menzel Gerhard, Braunschweig, Germany) (*see* **Note 7**).
8. Polystyrene 6-well Cell Culture Cluster (Corning B.V. Life Sciences, Schiphol-Rijk, Netherlands).
9. FuGENE6 transfection medium (Roche Molecular Biochemicals, Indianapolis, IN, USA). Store at 2–8°C.

2.3 Generation of Stable Cell Lines

1. Polystyrene tissue culture dishes 100×20 mm (Falcon; BDBiosciences, Alphen aan den Rijn, Netherlands).
2. Polystyrene 6-well cell culture cluster (Corning B.V. Life Sciences).
3. HyQ G418 sulfate (HyClone): working solution is 100 mg/mL active concentration in PBS. Final concentration in culture medium is 0.6 mg/mL (*see* **Note 6**).

2.4 Fluorescence Recovery After Photobleaching

1. All the quantitative FRAP procedures are performed on a Zeiss Confocal Laser Scanning Microscope LSM510 META equipped with a ×40/1.3A NA oil immersion objective, a Lasos LGK 7812 ML-4 Laser Class 3 B Argon laser (30 mW) with the excitation laser lines 458 and 488, and an acousto-optical tunable filter (AOTF) (Carl Zeiss MicroImaging, Jena, Germany) (*see* **Note 8**).
2. The filter set to specifically image GFP is shown in Table 20.1 (*see* **Note 4**).
3. Temperature is controlled by a heatable stage and a lens-heating device, both developed in our laboratory (*see* **Note 9**).
4. The LSM 5 software, Version 3.2 controls the microscope, the scanning and laser modules, and the image acquisition process. This software is also used to analyze the images.

Table 20.1 Filter sets used in FRAP experiments

Fluorophore	Excitation	Main beam splitter	Secondary beam splitter	Emission filter
EGFP	488 nm	HFT 488	Mirror	BP 505–530
ECFP	458 nm	HFT 458/514	NFT 515	BP 470–500
EYFP	514 nm	HFT 458/514	NFT 515	LP 560

3 Methods

3.1 Constructs

1. The GFP-AR coding construct is generated by performing PCR on pAR0 (39) using a sense primer (5′-GCAGAAGATCTGCAGGTGCTGGAGCAGGTGCT GGAGCAGGTGCTGGAGAAGTGCAGTTAG-3′) to introduce a *Bgl*II restriction site and a flexible $(GlyAla)_6$ spacer sequence and an anti-sense primer in the AR cDNA overlapping a *Sma*I site (5′-TTGCTGTTCCTCATCCAGGA-3′) (*see* **Note 10**).
2. The PCR product is cloned in pGEM-T-Easy and the sequence is verified.
3. The *Bgl*II-*Sma*I fragment is inserted in the corresponding sites of pEGFP-C1.
4. Next, the *Sma*I fragment from pAR0 is inserted into the *Sma*I site to generate pGFP-$(GlyAla)_6$-AR (further referred to as GFP-AR).
5. The non-DNA-binding mutant is obtained by exchanging the *Asp*718I-*Sca*I fragment from pAR(A573D) in GFP-AR.

3.2 Cell Culture and Cell Transfection (see Note 11)

1. Hep3B cells are grown in αMEM supplemented with L-glutamine, penicillin, streptomycin, and 5% FCS at 37°C and 5% CO_2 and passaged when approaching confluence (every 3–4 days) with trypsin/EDTA to provide experimental cultures.
2. Two days before confocal microscopy, Hep3B cells are seeded on a coverslip in a 6-well plate at a concentration of ~3×10^5 cells per well in 2 mL of αMEM with 5% FCS (*see* **Note 12**). This concentration will provide near-confluent cultures at the time of the experiment and a sufficient amount of cells at the time of transfection. The cells are grown overnight at 37°C with 5% CO_2.
3. Between 24 and 32 h before confocal microscopy, the medium is replaced by 1 mL of αMEM supplemented with 5% charcoal-stripped serum, L-glutamine and antibiotics, without washing the cells.
4. After 2 h the transfection mix is prepared for transfection of 1 µg of GFP-AR coding vector. Three microliters of FuGENE6 per microgram of DNA to be

transfected is added to 100 µL of serum-free αMEM. After 5 min incubation, the DNA is added. The transfection mix is then gently mixed by pipetting up and down, and left at room temperature for at least 30 min (*see* **Note 13**).
5. Four hours after medium replacement, the transfection mix is gently added to the cells under gentle mixing. The cells are then incubated for 4 h at 37°C and 5% CO_2.
6. Four hours after transfection the medium is replaced again by 2 mL of αMEM supplemented with charcoal-stripped serum with or without 1 n*M* R1881. The cells are further incubated overnight at 37°C and 5% CO_2.

3.3 Generation of Stable Cell Lines

To avoid transfections before each experiment and to simplify the selection of cells with physiologically relevant expression level of the tagged protein, a cell line stably expressing a receptor with fluorescent label(s) can be generated. It is often stated that the use of cells stably expressing fusion proteins is essential to avoid overexpression, but microscopic approaches enable preselection of cells with a physiological expression level also in transient transfected cells. With this in mind, also transiently transfected cells can be studied when a sufficient number of cells in the required expression range can be found (*see* **Note 11**).

1. Hep3B cells are seeded in 6 wells of a 6-well plate in αMEM with 5% FCS as described in Section 3.2, and incubated overnight at 37°C and 5% CO_2.
2. After overnight incubation, the cells in all 6 wells are transfected with the same expression vector (1 µg of DNA for each well) as described in Section 3.2.
3. Four hours after transfection, the medium is replaced by 2 mL of αMEM/5% FCS and the cells are incubated overnight at 37°C and 5% CO_2.
4. After overnight incubation the cells are trypsinised and an array of dilutions ranging from 9:10 to 1:1,000 are seeded in 10-cm-diameter dishes. The Hep3B cells are incubated again overnight at 37°C and 5% CO_2.
5. After another overnight incubation the medium is replaced by αMEM with 5% FCS supplemented with 0.6 mg/mL of G418 (active concentration). The cells are further incubated at 37°C/5% CO_2. Twice a week, the medium is replaced by fresh medium with G418.
6. When the clones grown from single cells consist of 100–200 cells, the locations of the colonies are indicated with a fine marker underneath the bottom of the dish. Using a 200-µL pipette, each clone is carefully scraped while slowly collecting the cells by pipetting.
7. The collected cells are seeded in a glass-bottomed 24-well dish in 1 mL of αMEM with G418 and incubated for 1 or 2 weeks.
8. When the clones have grown, the expression of GFP-AR is judged by confocal microscopy. The clones with sufficient expression are passaged and used for experiments (*see* **Note 14**).

3.4 Fluorescence Recovery After Photobleaching

3.4.1 Strip-FRAP

In the most elementary FRAP experiment, a small circular area that is illuminated by a stationary laser beam (the diffraction-limited spot) is bleached and the recovery of fluorescence inside the spot is monitored in time ***(14)***. The use of a confocal scanning microscope makes it possible to bleach larger areas by scanning at high intensity. In addition, not only the recovery of fluorescence in the bleached area, but also the fluorescence in the entire nucleus can be monitored.

There may be several potential drawbacks of bleaching a small area. First, the recovery of fluorescence is very fast, possibly too fast for the imaging system, especially when the entire nucleus is imaged. Second, the amount of fluorescence emitted by the limited number of molecules in a single spot is relatively low, leading to low signal-to-noise levels. Third, the relative location of the bleached spot inside the nucleus may influence the recovery curve. Therefore, we provide a FRAP protocol, designated strip-FRAP, in which a narrow is strip is bleached with a width of ~700 nm (corresponding to 10 pixels at zoom 6 on a Zeiss LSM 510 microscope) and spanning the entire nucleus. To assure a sufficient time resolution to also follow fast diffusion processes (like diffusion of free GFP), only the fluorescence in the bleached strip is monitored after photobleaching (Figs. 20.1a and 20.4a, c).

1. These instructions assume use of a Zeiss CLSM 510 confocal laser scanning microscope. For GFP-imaging in general, an argon laser is used, adjusted to 6.1-A tube current and allowed to prewarm for at least 15 min.
2. For live cell imaging, an inverted microscope is used. Cells are grown on a coverslip that forms the bottom of a container enabling the addition of medium on top of the cells. In the examples given here we investigated Hep3B cells expressing GFP-tagged androgen receptor (GFP-AR). The glass-bottom container containing the cells and medium is transferred into a heatable stage holder at 37°C (*see* **Note 9**), which is mounted on a motorized scan stage.
3. GFP-fluorescence is detected using 488-nm excitation, usually by an argon laser, using a 488-nm beam splitter and a band-pass emission filter passing GFP emission at 505–530 nm (Table 20.1) (*see* **Note 4**). Cells are imaged using a ×40/1.3 NA oil objective. The confocal pinhole is adjusted such that the estimated optical slice thickness is ~2 μm (corresponding to 2.48 Airy units).
4. Scanning is performed unidirectional with scan speed 9 to enable fast recording of the fluorescent signal in the strip. Laser intensity is attenuated to approximately 1% of the maximum output using an AOTF for scanning (~0.5–0.8 μW). Detector gain is set on 900, the amplifier offset on 0, and the amplifier gain on 1. Fluorescent signals are recorded with an 8-bit data depth (*see* **Notes 15–17**).
5. A nucleus expressing GFP-AR at physiologically relevant expression level (see **Note 18**) is selected at zoom 1 (*see* **Note 19**). To limit potential effects of nuclear shape, all nuclei are oriented in the same way relative to the bleaching strip (in our experiments we make sure that the longer axis of the more-or-less ellipsoid-shaped

nucleus is perpendicular to the strip. When the nucleus is oriented correctly, zoom is adjusted to 6 corresponding to a lateral pixel distance of 70 nm. A 10-pixel-wide (700-nm) strip spanning the nucleus is selected in the Edit ROI panel, for recording the recovery of the signal (Fig. 20.1a) (*see* **Note 20**).

6. The fluorescent signal is monitored at 21-msec intervals by scanning the region of interest (ROI) for 4000 iterations (~80 sec) prior to bleaching (Time Series Control) at low excitation (*see* **Note 21**). After 200 scans, GFP is bleached locally inside the ROI using a scan (1 or 2 iterations) at maximum intensity (Fig. 20.1a). The time-series are initiated using the Mean ROI option in the time-series control (*see* **Notes 22** and **23**).
7. After the scan the data can be copied directly to Excel or the file can be saved as a data-file for later analysis.

3.4.2 FLIP-FRAP

Next to the comparison of FRAP curves obtained from proteins under different experimental conditions, it may be useful to apply two different FRAP variants to a protein under the same conditions. For instance, the combination of strip-FRAP (Fig. 20.1a, b) and combined FLIP-FRAP (Fig. 20.1c, d) can be used to investigate transient immobilization ***(6, 13, 16)***. This approach is based on the fact that often more than one scenario (with different diffusion coefficient, immobile fraction, and time of immobilization) fits the experimental data. To differentiate between different scenarios that fit well to the results of a strip-FRAP experiment, it is possible to perform a complementary combined FLIP-FRAP experiment (Fig. 20.1c, d) since two different scenarios that result in similar curves in a strip-FRAP experiment give clearly different curves in a complementary FLIP-FRAP experiment ***(13)***. In FLIP-FRAP, the recovery of the fluorescence in a region at one end of the nucleus after bleaching for a relative long period (FRAP) is measured in parallel with the decrease of the signal in a similar region at the other pole of the nucleus (FLIP) (Fig. 20.1c, d). As stated above, the combination of strip-FRAP and FLIP-FRAP is especially applicable for studying transient immobilization as found for proteins (Fig. 20.4) ***(6, 7)***.

1. Confocal settings are similar to those used in the strip-FRAP procedure (steps 1–3) except for the Detector Gain, which is set on 1,000.
2. A 20-pixel-wide ROI spanning the nucleus at one pole is selected in the Edit ROI panel, for recording the recovery of the signal after bleaching. Using the Define Region option of the Bleach Control panel, the same ROI is selected to locally bleach GFP. A second ROI of similar width is selected spanning the nucleus at the other pole where the decrease of fluorescence due to redistribution of the proteins from the bleached area is measured (Fig. 20.1c). The distance between the two regions should be kept constant in different cells.

3. The fluorescent signal is monitored by scanning the two regions of interest for 35 iterations (approx. 100 sec) at a low excitation level with a 3-sec time interval (Time Series Control) (*see* **Note 21**). After the first scan the GFP is bleached locally inside the lowest ROI using 10 iterations of 488 nm laser light at maximum voltage (Fig. 20.1c). The time-series are initiated using the mean ROI option in the time-series control (*see* **Notes 22** and **23**).
4. After the scan the data can be copied directly to Excel or the file can be saved as a data-file for later analysis.

3.4.3 Qualitative FRAP Analysis

FRAP data can initially be qualitatively analyzed by comparing data from experiments applied when the protein under investigation is active or inactive. In the case of the study of steroid receptors like the AR, comparison of non-DNA-binding mutant versions and the wild type is possible where the differences observed between these can be ascribed to DNA binding. In our studies, direct comparison of a wild-type or mutant AR to a non-DNA-binding mutant (e.g. AR [A573D]) greatly simplifies the interpretation of the data, because this mutant is not immobilized (Fig. 20.2) ***(6, 7, 44)***.

In strip-FRAP the recovery of fluorescence in a narrow strip spanning the nucleus is scanned at low laser intensity after shortly bleaching the fluorescence inside this region (Fig. 20.1a, b). The qualitative comparison between FRAP curves from different experimental conditions requires some kind of normalization of the data. There are several ways to normalize FRAP data, each of which enables the extraction of different parameters (Fig. 20.2b–d) ***(13)***.

1. The most straightforward normalization of FRAP data is to express intensities relative to the average of a sufficient number of measurements before bleaching ($I_{\text{prebleach}}$): $I_{\text{norm,t}} = (I_{\text{t}} - I_{\text{background}})/(I_{\text{prebleach}} - I_{\text{background}})$, where $I_{\text{background}}$ is the background signal (Fig. 20.2b) (*see* **Note 24**).
2. Straightforward normalization can be extended with the normalization to the fluorescence intensity directly after bleaching (I_0), by expressing intensity values relative to the intensity directly after bleaching as well as to the average prebleach intensity: $I_{\text{norm,t}} = (I_{\text{t}} - I_0)/(I_{\text{pre}} - I_0)$. This way of normalization enables the quick visual estimation of the size of a potentially present immobilized fraction (Fig. 20.2c) (*see* **Note 1**).
3. A third way of normalization is to express intensity values relative to the fluorescence after complete recovery (I_∞), and the intensity directly after bleaching (I_0): $I_{\text{norm,t}} = (I_{\text{t}} - I_0)/(I_\infty - I_0)$. This yields a curve running from 0 directly after bleaching, to 1 after final recovery, allowing direct comparison of apparent diffusion rates irrespective of a potentially present immobile fraction, since different final recoveries due to different immobile fraction are not visible. In addition, this normalization is also often used for quantitative analysis by fitting the data

to any equation that represents the diffusion process (and transient immobilization) (Fig. 20.2d) ***(13)***.

4. Combined FLIP-FRAP data can be analyzed by first calculating the fluorescence intensity difference between the FLIP-region and the FRAP-region: $I_{\text{FLIP-FRAP}} = (I_{\text{FLIP-ROI}} - I_{\text{FRAP-ROI}})$. Subsequently the intensity differences can be expressed relative to the highest difference, i.e. immediately after bleaching (Fig. 20.1d and Fig. 20.4d).

3.4.4 Quantitative FRAP Analysis

Quantitative analysis of FRAP is mostly performed by fitting experimental data to mathematical models. Many different models have been brought forward ranging from simplified models based on 1-D diffusion ***(20, 45)*** to very sophisticated 3-D models incorporating as many aspects of the FRAP experiment as possible ***(46–52)***. These approaches have shown to be very useful for quantitative FRAP analysis, a slight drawback being that for instance diffusion in ellipsoid volumes or conically shaped laser beams are relatively difficult to solve analytically. Another possible approach to quantitatively analyse FRAP results is to generate FRAP curves by Monte Carlo simulation of diffusion of individual molecules and their binding to immobile elements (representing chromatin binding) in an ellipsoidal volume (representing the nucleus) as well as the shape and intensity distribution of the applied laser beam (Fig. 20.3) ***(6, 17, 20)***. The strength of Monte Carlo simulation is that it generates the highly complicated outcome of a set of relatively simple mathematically definable rules, such as diffusion of single particles in an ellipsoid volume, the presence of nucleoli, or the typical shape and intensity distribution of a focused laser beam, which are hard to solve analytically. The drawback of Monte Carlo simulations is that they are very time-consuming.

1. In our simulations, the size of the ellipsoid representing the nuclear volume is based on the experimentally determined average size of the investigated nuclei.
2. At the start of a Monte Carlo simulation, all tagged proteins start at a random position inside an ellipsoid volume representing the nucleus (Fig. 20.3a). Subsequently, the simulation goes through cycles representing a minimum time span. Typically in our simulations the time step was 21 msec, corresponding to the time it takes to scan a 10-pixels-wide strip spanning the width of the nucleus one time.
3. Diffusion of single particles (representing GFP-tagged proteins) is simulated using the strikingly simple Einstein-Smoluchowski relationship for 3-D Brownian motion: $D = s^2/6T$, where D is the diffusion coefficient, s is the average distance moved by the particles, and T is the time span in which the particles move, in our strip-FRAP simulations, 20 msec (Fig. 20.3a). Simulation of Brownian motion of individual particles only involves the additional consideration that the equation predicts the average movement of all particles, whereas single particles will travel

over slightly different distances. Therefore, diffusion of each particle is simulated by displacing it over a certain distance (corresponding to a certain diffusion coefficient) plus or minus a small variation defined by a Gaussian with standard deviation σ, which represents the stepsize per unit time and is related to the diffusion coefficient according to the above equation: $\sigma = \sqrt{6 D \Delta t}$. In practice the step to be made by the molecule is split in three steps, in *x*-, *y*-, and *z*-direction, respectively: at each new time $t + \Delta t$, a new position $(x_{t+\Delta t}, y_{t+\Delta t}, z_{t+\Delta t})$ is derived for all mobile molecules from their current position (x_t, y_t, z_t) by $x_{t+\Delta t} = x_t + G(r_1)$, $y_{t+\Delta t} = y_t + G(r_2)$, and $z_{t+\Delta t} = z_t + G(r_3)$, where r_i is a random number $(0 \le r_i \le 1)$ chosen from a uniform distribution, and $G(r_i)$ is an inversed cumulative Gaussian distribution with $\mu = 0$ and $\sigma^2 = 6 D \Delta t$, where D is the diffusion coefficient. Note that the latter follows directly from the Einstein-Smulochowski equation, the average stepsize being equal to the standard deviation of the Gaussian distribution.

4. Binding to and releasing from immobile elements in the nucleus (like chromatin) can also be simulated by simple mathematical expressions (Fig. 20.3b). The probability for an immobile molecule to release is the most easy to explain since, in simple binding kinetics, this only depends on the affinity of the protein, yielding an equation defining the chance of a molecule to release: $P_{mobilise} = k_{off} = 1/T_{imm}$, where T_{imm} is the time spent in the immobile state expressed in number of time steps. If for instance the average immobilisation time is three time steps (60 msec in our typical strip-FRAP simulation), an immobile molecule will in each step have a chance of 1/3 to release, leading to an expected residence time of three steps. From this simple equation, the chance for a free molecule to become immobile can be calculated when one takes into account the fact that the ratio of immobile and mobile molecules is equal to the ratio between k_{on} and k_{off} (law of mass action): $k_{on}/k_{off} = F_{imm}/F_{mob}$, where F_{mob} is the number of mobile molecules and F_{imm} is the number of immobile molecules. The probability for each particle to become immobilized (representing chromatin binding) then is $P_{immobilise} = k_{on} = k_{off} \cdot F_{imm}/F_{mob}$. Since above we saw that $k_{off} = 1/T_{imm}$, the chance to immobilise can be expressed fully in terms of immobile fraction and immobilisation time, the two typical mobility parameters obtained from FRAP experiments: $P_{immobilise} = k_{on} = (F_{imm})/(T_{imm} \cdot F_{mob})$
5. For bleaching simulation we use experimentally derived 3-D laser intensity profiles, determining the probability for each molecule to get bleached considering their 3-D position relative to the laser beam (Fig. 20.3c). The 3-D laser intensity profile is derived from the bleach pattern in confocal image stacks of chemically fixed nuclei containing GFP that were exposed to a stationary laser beam at various intensities and varying exposure times.
6. For quantitative analysis of the FRAP data, raw FRAP curves are normalized to pre-bleach values and the best-fitting curve (by ordinary least squares) is selected from a large set of FRAP curves generated as described above in which three parameters representing mobility properties were varied: diffusion rate (ranging from, e.g. 0.04 to 25 μm²/sec), k_{on} and k_{off} (corresponding to immobile fractions of, e.g. 0, 10, 20, …, 90%) and time spent in the immobile state (e.g. 2, 4, 8, 16, 32, 64, 128, 256, 512, 1,024, ∞ sec).

4 Notes

1. In FRAP, a considerable fraction of the fluorescent proteins inside a nucleus will be irreversibly bleached during the bleach pulse, resulting in incomplete recovery of the fluorescent signal independent of any immobile fraction.
2. Next to a diffusion coefficient, an immobile fraction and a residence time in the immobile state can be derived from FRAP curves. It is also possible to describe the dynamic binding and release from immobile components of the nucleus in terms of immobilisation (k_{on}) and release rate (k_{off}). The ratio between k_{on} and k_{off} then is equal to the ratio between mobile and immobile fraction. The residence time is equal to the inverse of the release rate k_{off} (*see also* **Section 3.4.4**).
3. Analysis of FRAP or FLIP curves is more complicated, since the recovery or loss of fluorescence is a result of dissociation and association of tagged proteins ***(13)***.
4. The examples given here are all based on EGFP-tagged proteins. If ECFP, EYFP, or other fluorescent dyes are used, imaging protocols should be modified according to the fluorescent properties of the chosen dye (see Table 20.1).
5. Hep3B cells do not express endogenous AR, are easy to transfect, and are relatively large, enhancing microscopic analysis. When using other cell types the expression of endogenous nuclear receptors needs to be taken into account. Although many GFP-tagged proteins are functional, their functionality will usually be less than the wild type. Endogenously expressed proteins compete with the tagged version, thereby limiting its activity compared with when no endogenous protein is present. A potential threat to the use of cell lines lacking endogenous expression is the potential absence of specific cofactors that modulate or enhance the activity of the studied protein.
6. Antibiotics are potentially harmful and should always be treated with proper personal protection.
7. Coverslips should not be thicker than 0.16 mm, because of the high numerical aperture of some of the lenses of the confocal microscope.
8. The LSM 510 is a laser hazard class 3 B instrument and is marked as such. This moderate-risk class includes medium-power lasers. You must take care not to expose yourself to the radiation of such lasers.
9. We use temperature-control equipment developed in our laboratory. Alternatively, commercially available equipment can be used varying from heatable plates up to complete incubators mounted on the microscope.
10. The insertion of a flexible stretch, for instance a short glycine–alanine repeat, between the protein of interest and the fluorescent label may decrease the potential (negative) effect of the label on the functionality of the protein of interest. For tagged ARs, most often reporter assays using androgen-regulated luciferase reporter genes are used to verify the functionality (6).
11. Although the use of cell lines stably expressing the tagged protein has a number of advantages, it may under circumstances be more convenient to investigate transiently transfected cells. In these cases it is important to only select cells that do not overexpress the protein. This can be achieved by, for example,

selecting cells at the same settings as used for stably expressing cells. Using these settings, fluorescence levels should be similar to cells stably expressing the protein at physiological levels. Fluorescence of overexpressing cells will be at the maximum in the entire nucleus (each pixel will have maximum intensity, in 8-bit imaging corresponding to a value of 255).

12. Coverslips in 6-well plates are sterilized by 45 min of UV treatment. Alternatively, they are submerged in ethanol and flamed before placing in the 6-well plate.
13. Do not vortex the transfection mix (refer to the FuGENE6 Transfection Reagent Instruction Manual). Contact between the undiluted FuGENE6 and any plastic surface (except for the pipette tip) should be avoided.
14. Alternatively, modern FACS-sorters could be used to select single cells on the basis of their fluorescent level, representing the expression level of the tagged protein. Each cell can be deposited in a separate well of, for instance, a 96-well plate. After incubation, the clones can be selected that have the appropriate expression level (step 7–8 above).
15. Although a higher detector gain (DG) is favorable to obtain higher signals, it increases noise. Therefore, a trade-off of settings to reduce both noise (e.g. lower DG, averaging) and monitor bleaching (e.g. lower excitation level, rapid scanning) but still giving high enough signal in low-expressing cells is necessary to optimize the experimental setup (e.g. wider pin-hole, higher DG, higher excitation level). These settings may also depend on the level or pattern of expression of the protein of interest. In general, for FRAP excitation laser intensity should be as low as possible, to avoid monitor bleaching, which is hard to correct for ***(13)*** (*see* **Note 16**).
16. The rate at which monitor bleaching occurs can be determined in a non-bleached area of the nucleus or by performing a FRAP experiment without applying the bleach pulse. Subsequently, experimental FRAP curves can be corrected according to the observed monitor bleach rate. However, when a significant immobile fraction is present, this fraction will contribute more to the monitor bleaching in the control measurements, than the mobile fraction, since immobile molecules stay constantly in the illuminated area, whereas mobile ones move in and out. In a FRAP experiment this immobile fraction is largely bleached, leading to less monitor bleaching after photobleaching than estimated on the basis of the control curves. Thus, the presence of a (transiently) immobile fraction will lead to overcorrection of the experimental curve and subsequent underestimation or failure to detect this fraction. Therefore, it is important to avoid monitor bleaching or to limit it as much as possible.
17. Settings for imaging in the LSM510 software must be selected in several panels; Scan Control, Edit ROI, Time Series Control, and Bleach Control. Settings for imaging are selected using the Scan and Time Series control menus.
18. For all the approaches discussed, it is essential to select cells with physiologically relevant expression levels. Overexpression can lead to aggregation and artificial immobilization of the receptors (53). For quantitative measurements like FRAP described here, high-resolution imaging is not essential.

19. To speed up the procedure it is advisable to use software to put the center of the nucleus in the middle of the scanning area ("center" macro in the macro-directory).
20. It is not essential to use the exact values given here, but the values chosen should be kept constant (similar) over sets of experiments to allow comparison between curves of different proteins/conditions.
21. It is important to limit monitor bleaching by applying excitation at a low laser power. Although monitor bleaching correction procedures are designed for FRAP experiments, it is favorable to limit the monitor bleaching during data collection.
22. By selecting the Mean ROI option in the time series control panel, only the mean intensity inside the ROI is plotted. In contrast, by selecting StartB (or StartT) all scans of the ROI are saved for later analysis.
23. In the configuration, the monitor diode (ChM) can be selected also to monitor potential fluctuations of laser intensity during scanning, and used afterwards for correction. Note that lasers become less stable towards the end of their life.
24. In data normalisation where the intensity after bleaching is set to 0, some information is lost, since the depth of the bleach pulse is not only determined by laser intensity but also by protein mobility and size of the immobile fraction: the slower the protein and the larger the immobile fraction, the deeper the bleach pulse will be. If experimental curves are fit to models that take into account bleach depth, the estimates of D, k_{on}, and k_{off}, (or immobile fraction and residence time in the immobile state) may be more accurate than when bleach depth is not taken into account.
25. Although in many FRAP analyses it is assumed that proteins are irreversibly photobleached, it has been shown that a fraction of proteins will regain their fluorescence, a process often referred to as blinking. Blinking not only occurs when GFP is illuminated at high intensity for photobleaching, but also at lower monitor intensities, although the time spent in the fluorescent state (on-time) of blinking GFPs is shorter at higher intensities. In contrast, the off-times are independent of excitation intensity ***(54)***. Therefore, in a FRAP-experiment the fraction of GFPs in the reversible off-state will increase during the high intensity bleach pulse, and decrease again during subsequent monitoring at low intensity, leading to a recovery of fluorescence that is not related to protein mobility. Although the contribution of this will be limited if molecules are relatively mobile, in cases where the majority or all of the investigated proteins are immobile (for instance core histones) the effect will be substantial, leading to underestimation of the immobile fraction.

References

1. Tsien, R. Y. (1998) The green fluorescent protein. *Ann. Rev. Biochem.* **67**, 509–544.
2. Lippincott-Schwartz, J. and Patterson, G. H. (2003) Development and use of fluorescent protein markers in living cells. *Science* **300**, 87–91.
3. Shaner, N. C., Steinbach, P. A., and Tsien, R. Y. (2005) A guide to choosing fluorescent proteins. *Nat. Meth.* **2**, 905–909.

4. Heim, R. and Tsien, R. Y. (1996) Engineering green fluorescent protein for improved brightness, longer wavelengths and fluorescence resonance energy transfer. *Curr. Biol*. **6**, 178–182.
5. Giepmans, B. N. G., Adams, S. R., Ellisman, M. H., and Tsien, R. Y. (2006) The fluorescent toolbox for assessing protein location and function. *Science* **312**, 217–224.
6. Farla, P., Hersmus, R., Geverts, B., Mari, P. O., Nigg, A. L., Dubbink, H. J., Trapman, J., and Houtsmuller, A. B. (2004) The androgen receptor ligand-binding domain stabilizes DNA binding in living cells. *J. Struct. Biol*. **147**, 50–61.
7. Farla, P., Hersmus, R., Trapman, J., and Houtsmuller, A. B. (2005) Antiandrogens prevent stable DNA-binding of the androgen receptor. *J. Cell Sci*. **118**, 4187–4198.
8. Rayasam, G. V., Elbi, C., Walker, D. A., Wolford, R., Fletcher, T. M., Edwards, D. P., and Hager, G. L. (2005) Ligand-specific dynamics of the progesterone receptor in living cells and during chromatin remodeling in vitro. *Mol. Cell. Biol*. **25**, 2406–2418.
9. McNally, J. G., Müller, W. G., Walker, D., Wolford, R., and Hager, G. L. (2000) The glucocorticoid receptor: rapid exchange with regulatory sites in living cells. *Science* **287**, 1262–1265.
10. Schaaf, M. J. and Cidlowski, J. A. (2003) Molecular determinants of glucocorticoid receptor mobility in living cells: the importance of ligand affinity. *Mol. Cell. Biol*. **23**, 1922–1934.
11. Stenoien, D. L., Patel, K., Mancini, M. G., Dutertre, M., Smith, C. L., O'Malley, B. W., and Mancini, M. A. (2001) FRAP reveals that mobility of oestrogen receptor-alpha is ligand- and proteasome-dependent. *Nat. Cell Biol*. **3**, 15–23.
12. Agresti, A., Scaffidi, P., Riva, A., Caiolfa, V. R., and Bianchi, M. E. (2005) GR and HMGB1 interact only within chromatin and influence each other's residence time. *Mol. Cell* **18**, 109–121.
13. Houtsmuller, A. B. (2005) Fluorescence recovery after photobleaching: application to nuclear proteins. In: *Advances in biochemical engineering* (Rietdorf, J., Ed.), Vol. 95, Springer-Verlag, Berlin, pp. 177–199.
14. Axelrod D, K. D., Schlessinger J, Elson E, and Webb WW. (1976) Mobility measurement by analysis of fluorescence photobleaching recovery kinetics. *Biophys. J*. **16**, 1055–1069.
15. Fukano, T., Hama, H., and Miyawaki, A. (2004) Similar diffusibility of membrane proteins across the axon-soma and dendrite-soma boundaries revealed by a novel FRAP technique. *J. Struct. Biol*. **147**, 12–18.
16. Houtsmuller, A. B. and Vermeulen, W. (2001) Macromolecular dynamics in living cell nuclei revealed by fluorescence redistribution after photobleaching. *Histochem. Cell Biol*. **115**, 13–21.
17. Hoogstraten, D., Nigg, A. L., Heath, H., Mullenders, L. H. F., van Driel, R., Hoeijmakers, J. H. J., Vermeulen, W., and Houtsmuller, A. B. (2002) Rapid switching of TFIIH between RNA polymerase I and II transcription and DNA repair in vivo. *Mol. Cell* **10**, 1163–1174.
18. Mattern, K. A., Swiggers, S. J., Nigg, A. L., Lowenberg, B., Houtsmuller, A. B., and Zijlmans, J. M. (2004) Dynamics of protein binding to telomeres in living cells: implications for telomere structure and function. *Mol. Cell. Biol*. **24**, 5587–5594.
19. Dundr, M., Hoffmann-Rohrer, U., Hu, Q., Grummt, I., Rothblum, L. I., Phair, R. D., and Misteli, T. (2002) A kinetic framework for a mammalian RNA polymerase in vivo. *Science* **298**, 1623–1626.
20. Houtsmuller, A. B., Rademakers, S., Nigg, A. L., Hoogstraten, D., Hoeijmakers, J. H. J., and Vermeulen, W. (1999) Action of DNA repair endonuclease ERCC1/XPF in living cells. *Science* **284**, 958–961.
21. Rademakers, S., Volker, M., Hoogstraten, D., Nigg, A. L., Mone, M. J., van Zeeland, A. A., Hoeijmakers, J. H. J., Houtsmuller, A. B., and Vermeulen, W. (2003) Xeroderma pigmentosum group A protein loads as a separate factor onto DNA lesions. *Mol. Cell. Biol*. **23**, 5755–5767.
22. Sporbert, A., Gahl, A., Ankerhold, R., Leonhardt, H., and Cardoso, M. C. (2002) DNA polymerase clamp shows little turnover at established replication sites but sequential de novo assembly at adjacent origin clusters. *Mol. Cell* **10**, 1355–1365.
23. Essers, J., Theil, A. F., Baldeyron, C., van Cappellen, W. A., Houtsmuller, A. B., Kanaar, R., and Vermeulen, W. (2005) Nuclear dynamics of PCNA in DNA replication and repair. *Mol. Cell. Biol*. **25**, 9350–9359.
24. Zotter, A., Luijsterburg, M. S., Warmerdam, D. O., Ibrahim, S., Nigg, A., van Cappellen, W. A., Hoeijmakers, J. H. J., van Driel, R., Vermeulen, W., and Houtsmuller, A. B. (2006)

Recruitment of the nucleotide excision repair endonuclease XPG to sites of UV-induced DNA damage depends on functional TFIIH. *Mol. Cell. Biol*. **26**, 8868–8879.
25. Phair, R. D. and Misteli, T. (2000) High mobility of proteins in the mammalian cell nucleus. *Nature* **404**, 604–609.
26. Phair, R. D., Scaffidi, P., Elbi, C., Vecerova, J., Dey, A., Ozato, K., Brown, D. T., Hager, G., Bustin, M., and Misteli, T. (2004) Global nature of dynamic protein-chromatin interactions in vivo: three-dimensional genome scanning and dynamic interaction networks of chromatin proteins. *Mol. Cell. Biol*. **24**, 6393–6402.
27. Essers, J, Houtsmuller, A. B., van Veelen, L., Paulusma, C., Nigg, A. L., Pastink, A., Vermeulen, W., Hoeijmakers, J. H., and Kanaar, R. (2002) Nuclear dynamics of RAD52 group homologous recombination proteins in response to DNA damage. *EMBO J*. **21**, 2030–2037.
28. Lukas, C., Falck, J., Bartkova, J., Bartek, J., and Lukas, J. (2003) Distinct spatiotemporal dynamics of mammalian checkpoint regulators induced by DNA damage. *Nat. Cell Biol*. **5**, 255–260.
29. Lukas, C., Melander, F., Stucki, M., Falck, J., Bekker-Jensen, S., Goldberg, M., Lerenthal, Y., Jackson, S., Bartek, J., and Lukas, J. (2004) Mdc1 couples DNA double-strand break recognition by Nbs1 with its H2AX-dependent chromatin retention. *EMBO J*. **23**, 2674–2683.
30. Bekker-Jensen, S., Lukas, C., Melander, F., Bartek, J., and Lukas, J. (2005) Dynamic assembly and sustained retention of 53BP1 at the sites of DNA damage are coordinated by Mdc1/NFBD1. *J. Cell Biol*. **170**, 201–211.
31. Leonhardt, H., Rahn, H.-P., Weinzierl, P., Sporbert, A., Cremer, T., Zink, D., and Cardoso, M. C. (2000) Dynamics of DNA replication factories in living cells. *J. Cell Biol*. **149**, 271–280.
32. Kimura, H. and Cook, P. R. (2001) Kinetics of core histones in living human cells: little exchange of H3 and H4 and some rapid exchange of H2B. *J. Cell Biol*. **153**, 1341–1354.
33. Kimura, H. (2005) Histone dynamics in living cells revealed by photobleaching. *DNA Rep. (Amst.)* **4**, 939–950.
34. Chen, D., Dundr, M., Wang, C., Leung, A., Lamond, A., Misteli, T., and Huang, S. (2005) Condensed mitotic chromatin is accessible to transcription factors and chromatin structural proteins. *J. Cell Biol*. **168**, 41–54.
35. Kruhlak, M. J., Lever, M. A., Fischle, W., Verdin, E., Bazett-Jones, D. P., and Hendzel, M. J. (2000) Reduced mobility of the alternate splicing factor (ASF) through the nucleoplasm and steady state speckle compartments. *J. Cell Biol*. **150**, 41–52.
36. Kimura, H., Sugaya, K., and Cook, P. R. (2002) The transcription cycle of RNA polymerase II in living cells. *J. Cell Biol*. **159**, 777–782.
37. Trapman, J. (2001) Molecular mechanisms of prostate cancer. *Eur. J. Cancer* **37**, S119–125.
38. Feldman, B. J. and Feldman, D. (2001) The development of androgen-independent prostate cancer. *Nat. Rev. Cancer* **1**, 34–45.
39. Brinkmann, A. O., Faber, P. W., van Rooij, H. C. J., Kuiper, G. G. J. M., Ris, C., Klaassen, P., van der Korput, J. A. G. M., Voorhorst, M. M., van Laar, J. H., Mulder, E., and Trapman, J. (1989) The human androgen receptor: domain structure, genomic organization and regulation of expression. *J. Steroid Biochem*. **34**, 307–310.
40. Claessens, F., Verrijdt, G., Schoenmakers, E., Haelens, A., Peeters, B., Verhoeven, G., and Rombauts, W. (2001) Selective DNA binding by the androgen receptor as a mechanism for hormone-specific gene regulation. *J. Steroid Biochem. Mol. Biol*. **76**, 23–30.
41. Cleutjens, K. B. J. M., van der Korput, J. A. G. M., van Eekelen, C. C. E. M., van Rooij, H. C. J., Faber, P. W., and Trapman, J. (1997) An androgen response element in a far upstream enhancer region is essential for high, androgen-regulated activity of the prostate-specific antigen promoter. *Mol. Endocrinol*. **11**, 148–161.
42. Schaaf, M. J. M., Lewis-Tuffin, L. J., and Cidlowski, J. A. (2005) Ligand-selective targeting of the glucocorticoid receptor to nuclear subdomains is associated with decreased receptor mobility. *Mol. Endocrinol*. **19**, 1501–1515.

43. Van Royen, M. E., Cunha, S. M., Brink, M. C., Mattern, K. A., Nigg, A. L., Dubbink, H. J., Verschure, P. J., Trapman, J., and Houtsmuller, A. B. (2007) Compartmentalization of androgen receptor protein-protein interactions in living cells. *J. Cell Biol*. **177**, 63–72.
44. Bruggenwirth, H. T., Boehmer, A. L. M., Lobaccaro, J. M., Chiche, L., Sultan, C., Trapman, J., and Brinkmann, A. O. (1998) Substitution of Ala564 in the first zinc cluster of the deoxyribonucleic acid (DNA)-binding domain of the androgen receptor by Asp, Asn, or Leu exerts differential effects on DNA binding. *Endocrinology* **139**, 103–110.
45. Ellenberg, J., Siggia, E. D., Moreira, J. E., Smith, C. L., Presley, J. F., Worman, H. J., and Lippincott-Schwartz, J. (1997) Nuclear membrane dynamics and reassembly in living cells: targeting of an inner nuclear membrane protein in interphase and mitosis. *J. Cell Biol*. **138**, 1193–1206.
46. Blonk, J. C. G., A. Don, H. Van Aalst, and J. J. Birmingham (1993) Fluorescence photobleaching recovery in the confocal scanning light microscope. *J. Micros*. **169**, 363–374.
47. Braga, J., Desterro, J., and Carmo-Fonseca, M. (2004) Intracellular macromolecular mobility measured by fluorescence recovery after photobleaching with confocal laser scanning microscopes. *Mol. Biol. Cell* **15**, 4749–4760.
48. Braga, J., McNally, J. G., and Carmo-Fonseca, M. (2007) A reaction-diffusion model to study RNA motion by quantitative fluorescence recovery after photobleaching. *Biophys. J*. **92**, 2694–2703.
49. Sprague, B. L., and McNally, J. G. (2005) FRAP analysis of binding: proper and fitting. *Trends Cell Biol*. **15**, 84–91.
50. Sprague, B. L., Pego, R. L., Stavreva, D. A., and McNally, J. G. (2004) Analysis of binding reactions by fluorescence recovery after photobleaching. *Biophys. J*. **86**, 3473–3495.
51. Braeckmans, K., Peeters, L., Sanders, N. N., De Smedt, S. C., and Demeester, J. (2003) Three-dimensional fluorescence recovery after photobleaching with the confocal scanning laser microscope. *Biophys. J*. **85**, 2240–2252.
52. Carrero, G., McDonald, D., Crawford, E., de Vries, G., and Hendzel, M. J. (2003) Using FRAP and mathematical modeling to determine the in vivo kinetics of nuclear proteins. *Methods* **29**, 14–28.
53. Marcelli, M., Stenoien, D. L., Szafran, A. T., Simeoni, S., Agoulnik, I. U., Weigel, N. L., Moran, T., Mikic, I., Price, J. H., and Mancini, M. A. (2006) Quantifying effects of ligands on androgen receptor nuclear translocation, intranuclear dynamics, and solubility. *J. Cell. Biochem*. **98**, 770–788.
54. Garcia-Parajo, M. F., Segers-Nolten, G. M. J., Veerman, J.-A., Greve, J., and van Hulst, N. F. (2000) Real-time light-driven dynamics of the fluorescence emission in single green fluorescent protein molecules. *Proc. Natl. Acad. Sci. USA* **97**, 7237–7242.